

Lead-tellurium oxysalts from Otto Mountain near Baker, California: III. Thorneite, $\text{Pb}_6(\text{Te}_2^{6+}\text{O}_{10})(\text{CO}_3)\text{Cl}_2(\text{H}_2\text{O})$, the first mineral with edge-sharing octahedral tellurate dimers

ANTHONY R. KAMPF,^{1,*} ROBERT M. HOUSLEY,² AND JOSEPH MARTY³

¹Mineral Sciences Department, Natural History Museum of Los Angeles County, 900 Exposition Blvd., Los Angeles, California 90007, U.S.A.

²Division of Geological and Planetary Sciences, California Institute of Technology, Pasadena, California 91125, U.S.A.

³3457 E. Silver Oak Road, Salt Lake City, Utah 84108, U.S.A.

ABSTRACT

Thorneite, $\text{Pb}_6(\text{Te}_2^{6+}\text{O}_{10})(\text{CO}_3)\text{Cl}_2(\text{H}_2\text{O})$, is a new tellurate from Otto Mountain near Baker, California, named in honor of Brent Thorne. The new mineral occurs on fracture surfaces and in small vugs in brecciated quartz veins. Thorneite is directly associated with acanthite, cerussite, gold, hessite, iodargyrite, khinite, wulfenite, and three other new tellurates: housleyite, markcooperite, and ottoite. Various other secondary minerals occur in the veins, including three other new secondary tellurium minerals: paratimroseite, telluroperite, and timroseite. Thorneite is monoclinic, space group $C2/c$, $a = 21.305(1)$, $b = 11.059(1)$, $c = 7.564(1)$ Å, $\beta = 101.112(4)^\circ$, $V = 1748.8(4)$ Å³, and $Z = 4$. Crystals are prismatic to bladed with elongation and striations parallel to \mathbf{c} and typically occur in parallel and random aggregates. It is yellow and transparent, with pale yellow streak and adamantine luster. Mohs hardness is estimated at 2. The mineral is brittle, with an irregular to splintery fracture and good {100} cleavage. The calculated density is 6.828 g/cm³. Thorneite is biaxial (+), with large $2V$, but indices of refraction are too high to be measured. The optic orientation is $Y = \mathbf{b}$, $Z \wedge \mathbf{a} = 29^\circ$ in obtuse β . No pleochroism was observed. Electron microprobe analysis provided PbO 73.90, ZnO 0.03, TeO₃ 20.35, Cl 2.29, H₂O 1.28 (structure), CO₂ 2.29 (structure), O≡Cl −0.52, total 99.62 wt%; the empirical formula (based on O+Cl = 16) is $(\text{Pb}_{5.94}\text{Zn}_{0.01})(\text{Te}_{2.08}\text{O}_{10})(\text{C}_{1.00}\text{O}_3)[\text{Cl}_{1.16}\text{O}_{0.34}(\text{OH})_{0.50}](\text{H}_2\text{O})$. The strongest powder X-ray diffraction lines are [d_{obs} in Å (hkl) I]: 10.43 (200) 35, 3.733 ($\bar{5}11$, $\bar{2}02$, 002) 27, 3.595 ($\bar{4}21$) 33, 3.351 (112) 66, 3.224 (511, 131) 100, 3.093 ($\bar{2}22$, $\bar{3}31$) 30, 2.900 ($\bar{6}21$) 44, 2.133 (821, 622, 223, 731, 242) 38. The crystal structure ($R_1 = 0.028$) contains edge-sharing octahedral tellurate dimers, $[\text{Te}_2^{6+}\text{O}_{10}]^{8-}$ that bond to Pb atoms, which in turn are linked via bonds to Cl atoms, CO₃ triangles, and H₂O molecules.

Keywords: Thorneite, new mineral, tellurate, crystal structure, Otto Mountain, California

INTRODUCTION

Thorneite, $\text{Pb}_6(\text{Te}_2^{6+}\text{O}_{10})(\text{CO}_3)\text{Cl}_2(\text{H}_2\text{O})$, is one of seven new secondary lead-tellurium minerals discovered recently at Otto Mountain near Baker, California. Detailed information on the mining history, geology, mineralogy, and mineral paragenesis of the deposit, as well as the discovery of the new minerals, is provided in Kampf et al. (2010a).

Thorneite is named in honor of Brent Thorne (b. 1951) of Bountiful, Utah, the discoverer of the mineral. Brent Thorne is an avid field collector and regular contributor to Mindat.org with over 1100 photographs posted on the Mindat website. He has collected and provided specimens for the description of the new mineral plumbophyllite (Kampf et al. 2009) and for continuing studies of other new and existing minerals from Otto Mountain and the nearby Blue Bell claims. Thorne has agreed to the naming of the mineral in his honor. The new mineral and name have been approved by the Commission on New Minerals, Nomenclature and Classification of the International Mineralogical Association (IMA 2009-023). Four cotype specimens are deposited in

the Natural History Museum of Los Angeles County, catalog numbers 62257, 62258, 62259, and 62260.

OCCURRENCE

Thorneite was found in the Bird Nest drift on the southwest flank of Otto Mountain, approximately 2 km northwest of Baker, San Bernardino County, California. The Bird Nest drift (35° 16.606'N, 116° 05.956'W) is located 0.7 km northwest of the Aga mine (35° 16.399'N, 116° 05.665'W).

Thorneite is rare and occurs mostly on fracture surfaces and in small vugs in quartz veins. Species observed in direct association with the new mineral include acanthite, cerussite, gold, hessite, iodargyrite, khinite, wulfenite, and three other new tellurates: housleyite $[\text{Pb}_6\text{Cu}^{2+}\text{Te}_4^{6+}\text{O}_{18}(\text{OH})_2]$ (IMA2009-024; Kampf et al. 2010b), markcooperite $[\text{Pb}_2(\text{UO}_2)\text{Te}^{6+}\text{O}_6]$ (IMA2009-045; Kampf et al. 2010c), and ottoite $[\text{Pb}_2\text{Te}^{6+}\text{O}_5]$ (IMA2009-063; Kampf et al. 2010a). Other species identified in the Otto Mountain assemblages include: anglesite, atacamite, boleite, brochantite, burckhardtite, calcite, caledonite, celestine, chalcocopyrite, bromine-rich chlorargyrite, chrysocolla, devilline, diaboite, fluorite, fornacite, galena, goethite, jarosite, kuranakhite, linarite, malachite, mimetite, mottramite, munakataite, murdochite,

* E-mail: akampf@nhm.org

muscovite, perite, phosphohedyphane, plumbojarosite, pyrite, schiefelinite, vanadinite, vauquelinite, and three other new minerals: paratimroseite $[\text{Pb}_2\text{Cu}_3^{2+}(\text{Te}^{6+}\text{O}_6)_2(\text{H}_2\text{O})_2]$ (IMA2009-065; Kampf et al. 2010d), telluroperite $[\text{Pb}_3\text{Te}^{4+}\text{O}_4\text{Cl}_2]$ (IMA2009-044; Kampf et al. 2010e), and timroseite $[\text{Pb}_2\text{Cu}_3^{2+}(\text{Te}^{6+}\text{O}_6)_2(\text{OH})_2]$ (IMA2009-064; Kampf et al. 2010d). Other potentially new species are still under investigation.

Thorneite and most of the other secondary minerals of the quartz veins are interpreted as having formed from the partial oxidation of primary sulfides (e.g., galena) and tellurides (e.g., hessite) during or following brecciation of the quartz veins.

PHYSICAL AND OPTICAL PROPERTIES

The mineral occurs as prismatic to bladed crystals (Fig. 1) with elongation and striations parallel to *c*. They typically occur in parallel and random intergrowths and are up to 0.5 mm in length. Crystals exhibit the forms $\{100\}$, $\{010\}$, $\{110\}$, and $\{2\bar{1}\bar{1}\}$ (Fig. 2). Crystal intergrowths are common, but no systematic crystallographic orientation was observed.

Thorneite is yellow and transparent, with pale yellow streak and adamantine luster. The mineral is non-fluorescent. The Mohs hardness is estimated at 2 based upon behavior of crystals when broken. The tenacity is brittle and the fracture is irregular to splintery. Crystals are very fragile and easily crushed. Cleavage is good on $\{100\}$. The density could not be measured because it is greater than those of available high-density liquids and there is insufficient material for physical measurement. The calculated density is 6.790 g/cm³ for the empirical formula and 6.829 g/cm³ for formula based on refined occupancies in structure (see below). Thorneite turns opaque and dissolves slowly in HCl.



FIGURE 1. Backscatter SEM image of thorneite.

The indices of refraction exceed those of available index fluids. The Gladstone-Dale relationship (Mandarino 1981) predicts $n_{av} = 2.021$ based on the empirical formula. Birefringence is very low (~ 0.01), suggesting that all indices of refraction are in the 2.01 to 2.03 range. Orthoscopic and conoscopic optical examination using a Leitz Ortholux I polarizing microscope equipped with a Supper spindle stage showed thorneite to be biaxial (+), with large $2V$. No dispersion was observed. The optical orientation is $Y = \mathbf{b}$, $Z \wedge \mathbf{a} = 29^\circ$ in obtuse β . The mineral is non-pleochroic.

RAMAN SPECTROSCOPY

Raman spectroscopic micro-analysis was carried out using a Renishaw M1000 micro-Raman spectrometer system. Spectra were obtained using a 514.5 nm laser with a 100 \times objective producing a spot about 2 μm in diameter with about 5 mW power. Peak positions were calibrated against a silicon standard. Spectra were obtained with a dual-wedge polarization scrambler inserted directly above the objective lens to minimize the effects of polarization. Raman measurements were made on an isolated 150 $\mu\text{m} \times 50 \mu\text{m}$ thorneite crystal on quartz matrix. Spectra obtained with the light propagating parallel and perpendicular to the *c* axis of the crystal were found to be very similar. The spectra with the light propagating parallel to the *c* axis are shown in Figure 3a (100 to 1600 cm⁻¹ range) and Figure 3b (0 to 4000 cm⁻¹ range with the vertical scale expanded).

The sharp peak at 1056 cm⁻¹ is in the shift range where the strongest carbonate peak typically occurs. The broad peak at about 3300 cm⁻¹ is attributable to OH stretching modes and the peak at about 1630 cm⁻¹ is attributable to the HOH bending mode of water. The Raman spectroscopy, therefore, corroborates the presence of carbonate and water indicated by the structure determination (see below).

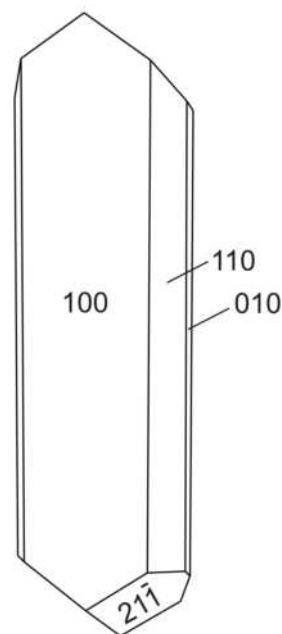


FIGURE 2. Crystal drawing of thorneite (clinographic projection).

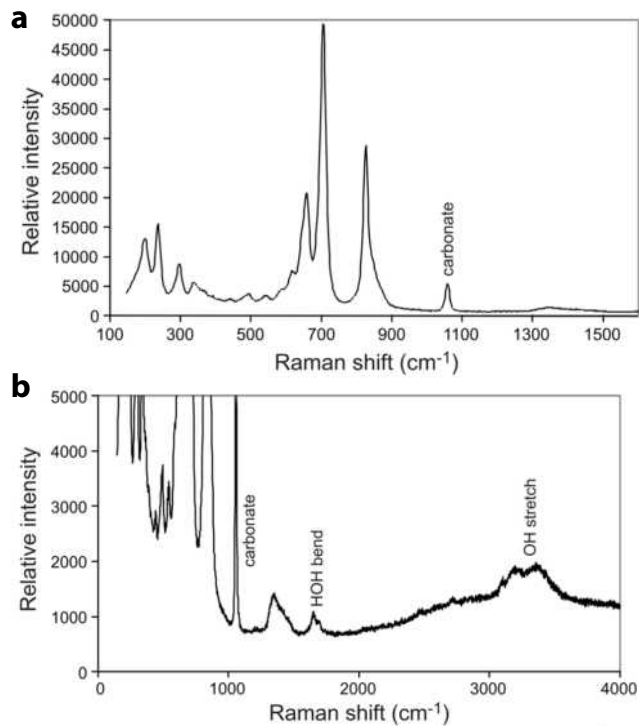


FIGURE 3. Raman spectra for thorneite (a) covering the range 100 to 1600 cm^{-1} and (b) covering the range 0 to 4000 cm^{-1} with expanded vertical scale.

CHEMISTRY

Three chemical analyses were carried out using a JEOL8200 electron microprobe (WDS mode, 15 kV, 10 nA, focused beam) at the Division of Geological and Planetary Sciences, California Institute of Technology. The H_2O and CO_2 were calculated by stoichiometry from the results of the crystal-structure analysis. The averages (and ranges) of the analyses are: PbO 73.90 (73.74–73.98), ZnO 0.03 (0.02–0.05), TeO_3 20.35 (20.05–20.76), Cl 2.29 (1.75–2.98), H_2O 1.26 (structure), CO_2 2.45 (structure), $\text{O}\equiv\text{Cl}$ –0.52, total 99.76 wt%. Standards used were PbS, ZnO, Te metal, and sodalite (for Cl). There was some evidence of beam damage during the EMP analyses; however, the final totals are close to 100% and the empirical formula derived from the analyses fits the structural formula well.

The empirical formula (based on $\text{O} + \text{Cl} = 16$) is $(\text{Pb}_{5.94}\text{Zn}_{0.01})(\text{Te}_{2.08}^{6+}\text{O}_{10})(\text{C}_{1.00}\text{O}_3)(\text{Cl}_{1.16}\text{O}_{0.34}(\text{OH})_{0.50})(\text{H}_2\text{O})$. The simplified formula is $\text{Pb}_6(\text{Te}_2^{6+}\text{O}_{10})(\text{CO}_3)(\text{Cl}_{1.50}(\text{OH})_{0.50})(\text{H}_2\text{O})$, based on the structure with refined Cl and OH occupancies for the Cl/OH site. The end-member formula is $\text{Pb}_6(\text{Te}_2^{6+}\text{O}_{10})(\text{CO}_3)\text{Cl}_2(\text{H}_2\text{O})$, which requires PbO 74.10, TeO_3 19.43, CO_2 2.44, H_2O 1.00, Cl 3.92, $\text{O}\equiv\text{Cl}$ –0.89, total 100.00 wt%.

X-RAY CRYSTALLOGRAPHY AND STRUCTURE DETERMINATION

Both powder and single-crystal X-ray diffraction data were obtained on a Rigaku R-Axis Spider curved imaging plate microdiffractometer utilizing monochromatized $\text{MoK}\alpha$ radiation. The powder data presented in Table 1 show good agreement with the pattern calculated from the structure determination.

TABLE 1. X-ray powder-diffraction data for thorneite

l_{obs}	d_{obs}	d_{calc}	l_{calc}	hkl
35	10.430	10.452	60	200*
14	9.740	9.775	25	110
6	5.550	5.529	14	020*
10	5.040	5.033	12	311*
13	4.940	4.888	12	220
6	4.440	4.434	9	021*
18	4.270	4.288	14	311*
10	3.900	3.911	16	510*
27	3.733	3.797	11	420
		3.750	11	511
		3.731	18	202*
		3.711	13	002
33	3.595	3.591	47	421*
		3.400	15	312
		3.370	38	112*
66	3.351	3.305	21	131
		3.302	14	202
		3.228	73	511*
100	3.224	3.219	100	131*
		3.093	26	222*
30	3.093	3.088	21	331*
21	2.969	2.973	31	512
		2.932	10	312
44	2.900	2.907	55	621*
		2.883	18	710
		2.874	23	711
		2.835	11	222
6	2.691	2.706	7	531
		2.673	10	240
		2.613	5	800
8	2.606	2.598	4	621
		2.591	7	041
6	2.581	2.444	8	440
12	2.428	2.427	18	313*
		2.363	4	820
8	2.361	2.362	12	802*
		2.292	4	223
3	2.285	2.221	6	242
6	2.226	2.220	7	423
		2.159	13	313
26	2.153	2.146	11	821
		2.144	16	622
		2.131	11	223
		2.126	20	731
4	2.075	2.120	14	242
		2.078	5	713
		2.060	5	351
		1.973	16	533*
15	1.969	1.966	8	802
		1.955	12	550
		1.875	5	1022
		1.873	9	1110*
15	1.863	1.866	9	404*
		1.858	7	913
		1.843	12	060
		1.798	10	552
		1.789	11	224
		1.780	9	642
22	1.782	1.777	17	750*
		1.773	9	243
		1.742	8	1200
3	1.737	1.737	4	533
		1.693	7	314
4	1.684	1.665	6	443
6	1.665	1.617	7	1042*
6	1.617	1.614	4	1022
		1.579	4	733
5	1.574	1.561	3	1221
10	1.555	1.561	9	244
		1.547	3	952
		1.497	7	1331*
12	1.493	1.496	5	371

Notes: l_{obs} based upon peak heights. l_{calc} calculated from the crystal structure using Powder Cell (Kraus and Nolze 1996). d_{calc} based on the cell refined from the powder data (*) using UnitCell (Holland and Redfern 1997). Refined cell: $a = 21.226(3)$, $b = 11.106(2)$, $c = 7.548(1)$ Å, $\beta = 101.33(2)^\circ$, $V = 1744.6(4)$ Å³.

The Rigaku CrystalClear software package was used for processing the structure data, including the application of an empirical absorption correction. The structure was solved by direct methods using SIR92 (Altomare et al. 1994) and the location of all non-hydrogen atoms was straightforward. The SHELXL-97 software (Sheldrick 2008) was used, with neutral atom scattering factors, for the refinement of the structure. Bond-valence calculations indicate that one O atom (designated OW) is a water molecule. A difference Fourier map revealed the H atom site corresponding to both H atoms of the water molecule. The position of the H site was constrained to an OW-H distance of 0.90(3) Å and an H-H distance of 1.45(3) Å in the final refinement. The structure refinement indicated the Cl site to be jointly occupied by Cl and OH [Cl_{0.75}(OH)_{0.25}]. It was not possible to locate the 0.25 H atom associated with this site.

The details of the data collection and the final structure refinement are provided in Table 2. The final atomic coordinates and displacement parameters are in Table 3. Selected interatomic

distances are listed in Table 4 and bond valences in Table 5. CIF and structure factors are on deposit¹.

DESCRIPTION OF THE STRUCTURE

The most distinctive unit in the structure (Fig. 4) is an edge-sharing octahedral tellurate dimer, [Te₂⁶⁺O₁₀]⁸⁻. The octahedral dimers bond to Pb atoms, which in turn are linked via bonds to Cl atoms, CO₃ triangles, and H₂O molecules. The thorneite structure is unique and is not closely related to that of any other mineral.

The average Te-O bond length in thorneite, 1.934 Å, is typical of octahedrally coordinated Te⁶⁺ [e.g., frankhawthorneite, 1.939 Å (Grice and Roberts 1995); jensenite, 1.936 Å (Grice et al. 1996); leisingite, 1.922 Å (Margison et al. 1997); khinite, 1.962 Å (Cooper et al. 2008); ottoite, 1.942 Å (Kampf et al. 2010a.); housleyite, 1.931 and 1.942 Å (Kampf et al. 2010b); markcooperite, 1.95 Å (Kampf et al. 2010c); timroseite, 1.933 Å

TABLE 2. Data collection and structure refinement details for thorneite

Diffractionmeter	Rigaku R-Axis Spider
X-ray radiation/power	MoK α ($\lambda = 0.71075$ Å)/50 kV, 40 mA
Temperature	298(2) K
Structural formula	Pb ₆ (Te ₂ ⁶⁺ O ₁₀)(CO ₃)(Cl _{1.50} (OH) _{0.50})(H ₂ O)
Space group	C2/c
Unit-cell dimensions	$a = 21.305(1)$ Å $b = 11.059(1)$ Å $c = 7.564(1)$ Å $\beta = 101.112(4)^\circ$
Z	4
Volume	1748.8(4) Å ³
Density (for above formula)	6.829 g/cm ³
Absorption coefficient	61.129 mm ⁻¹
F(000)	3016
Crystal size	85 × 70 × 15 μ m
θ range	3.46 to 23.24°
Index ranges	-23 ≤ h ≤ 23, -12 ≤ k ≤ 12, -7 ≤ l ≤ 8
Reflections collected/unique	8170/1255 [R _{int} = 0.0610]
Reflections with F _o > 4 σ F	1135
Completeness to $\theta = 27.50^\circ$	99.7%
Max. and min. transmission	0.4608 and 0.0782
Refinement method	Full-matrix least-squares on F ²
Parameters refined	120
GoF	1.069
Final R indices [F _o > 4 σ F]	R ₁ = 0.028, wR ₂ = 0.054
R indices (all data)	R ₁ = 0.033, wR ₂ = 0.055
Largest diff. peak/hole	1.395/-1.327 e/Å ³

Notes: R_{int} = $\sum |F_o^2 - F_c^2| / \sum F_o^2$. GoF = $S = \{ \sum [w(F_o^2 - F_c^2)]^2 / (n - p) \}^{1/2}$. R₁ = $\sum |F_o| - |F_c| / \sum F_o$. wR₂ = $\{ \sum [w(F_o^2 - F_c^2)]^2 / \sum [w(F_c^2)]^2 \}^{1/2}$. w = $1 / [\sigma^2(F_o^2) + (aP)^2 + bP]$, where a is 0, b is 107.075, and P is $[2F_o^2 + \text{Max}(F_c^2)]/3$.

TABLE 3. Atomic coordinates and displacement parameters (Å²) for thorneite

	x	y	z	U _{eq}	U ₁₁	U ₂₂	U ₃₃	U ₂₃	U ₁₃	U ₁₂
Pb1	0.63753(3)	0.09635(5)	0.15303(7)	0.0186(2)	0.0139(3)	0.0241(3)	0.0165(3)	-0.0012(2)	-0.0005(2)	0.0015(3)
Pb2	0.69515(3)	0.41296(5)	0.96922(8)	0.0220(2)	0.0218(4)	0.0233(3)	0.0195(3)	-0.0021(3)	0.0007(3)	-0.0020(3)
Pb3	0.55264(3)	0.24366(6)	0.52254(8)	0.0283(2)	0.0177(4)	0.0376(4)	0.0279(4)	-0.0047(3)	0.0006(3)	0.0056(3)
Te	0.78842(5)	0.30010(8)	0.36271(12)	0.0134(2)	0.0114(5)	0.0160(5)	0.0128(5)	-0.0008(4)	0.0024(4)	-0.0030(4)
C	0.5	0.9822(20)	0.25	0.025(6)	0.028(16)	0.017(13)	0.025(13)	0.0	-0.010(11)	0.0
Cl*	0.5884(3)	0.3933(6)	0.1682(8)	0.057(3)	0.032(4)	0.080(6)	0.059(5)	-0.002(3)	0.009(3)	0.006(3)
O1	0.5	0.0990(15)	0.25	0.052(5)	0.034(12)	0.033(11)	0.079(14)	0.0	-0.015(10)	0.0
O2	0.5487(6)	0.9265(11)	0.2183(17)	0.044(3)	0.022(7)	0.049(8)	0.063(9)	-0.009(7)	0.013(6)	0.001(6)
O3	0.7815(5)	0.4526(9)	0.2479(13)	0.026(3)	0.024(7)	0.028(6)	0.021(6)	0.008(5)	-0.006(5)	-0.011(5)
O4	0.6451(5)	0.2717(9)	0.7367(12)	0.020(2)	0.016(6)	0.028(6)	0.016(5)	-0.012(5)	0.003(5)	-0.008(5)
O5	0.7269(5)	0.2338(8)	0.1654(12)	0.016(2)	0.013(6)	0.019(6)	0.014(5)	0.004(4)	-0.004(4)	-0.004(4)
O6	0.6435(4)	0.1381(8)	0.4534(12)	0.014(2)	0.008(5)	0.025(6)	0.010(5)	-0.002(4)	0.003(4)	-0.001(4)
O7	0.7201(4)	0.3460(8)	0.4937(12)	0.012(2)	0.011(6)	0.013(5)	0.014(5)	-0.003(4)	0.008(4)	0.002(4)
OW	0.5	0.391(2)	0.75	0.089(8)	0.095(24)	0.094(20)	0.081(20)	0.0	0.022(17)	0.0
H	0.525(8)	0.442(5)	0.829(19)	0.08(8)						

* Refined Cl:OH occupancy: 0.75(4):0.25(4).

TABLE 4. Selected bond distances (Å) for thorneite

Te-O3	1.889(10)	Pb1-O6	2.297(9)
Te-O4	1.901(9)	Pb1-O3	2.360(10)
Te-O6	1.930(9)	Pb1-O5	2.423(9)
Te-O5	1.931(9)	Pb1-O2	2.777(12)
Te-O7	1.974(9)	Pb1-O6	3.016(9)
Te-O7	1.979(8)	Pb1-O1	3.155(1)
<Te-O>	1.934	Pb1-Cl	3.456(7)
		Pb1-O2	3.472(13)
C-O2(×2)	1.269(15)	Pb1-O4	3.728(10)
C-O1	1.291(26)	Pb1-O3	3.806(10)
<C-O>	1.276	<Pb1-O,Cl>	3.086
Pb2-O4	2.439(9)	Pb3-O4	2.317(10)
Pb2-O5	2.490(9)	Pb3-O6	2.404(9)
Pb2-O3	2.554(10)	Pb3-O2	2.406(12)
Pb2-O5	2.661(9)	Pb3-O1	2.679(10)
Pb2-O7	2.718(9)	Pb3-OW	2.758(16)
Pb2-Cl	2.968(6)	Pb3-Cl	3.360(6)
Pb2-O3	3.096(11)	Pb3-Cl	3.489(7)
Pb2-Cl	3.599(7)	Pb3-O2	3.699(12)
Pb2-O7	3.808(8)	Pb3-O7	3.788(9)
<Pb2-O,Cl>	2.991	<Pb3-O,Cl>	3.068

Hydrogen bonds (D = donor, A = acceptor)

D-H	d(D-H)	d(H-A)	D-H-A	d(D-A)	A	H-D-H
OW-H	0.92(3)	2.69(21)	114°	3.175(6)	Cl	104°
OW-H	0.92(3)	2.71(21)	128°	3.355(6)	Cl	

TABLE 5. Bond-valence analysis for thorneite

	O1	O2	O3	O4	O5	O6	O7	OW	Cl	Sum
Te			1.079	1.044	0.963	0.965	0.857, 0.846			5.754
C	1.307	1.387 ×2→								4.080
Pb1	0.088 ×2↓	0.190, 0.046	0.445, 0.023	0.027	0.391	0.506, 0.117			0.125	1.958
Pb2			0.299, 0.099	0.379	0.341, 0.241		0.214, 0.023		0.339, 0.094	2.029
Pb3	0.232 ×2↓	0.405, 0.029		0.486		0.407	0.024	0.197 ×2↓	0.152, 0.117	2.049
H								0.926	0.074	1.000
H'								0.931	0.069	1.000
Sum	1.946	2.057	1.945	1.936	1.936	1.994	1.964	2.252	0.970	

Notes: Values are expressed in valence units. Multiplicity is indicated by ×→↓; Pb²⁺-O bond strengths from Krivovichev and Brown (2001); Pb²⁺-Cl bond strengths from Brese and O'Keeffe (1991); Te⁶⁺-O bond strengths and hydrogen-bond strengths based on H...Cl/H...O bond lengths from Brown and Altermatt (1985); bond strength for Cl site assigned in accord with refined site occupancy [Cl_{0.75}(OH)_{0.25}].

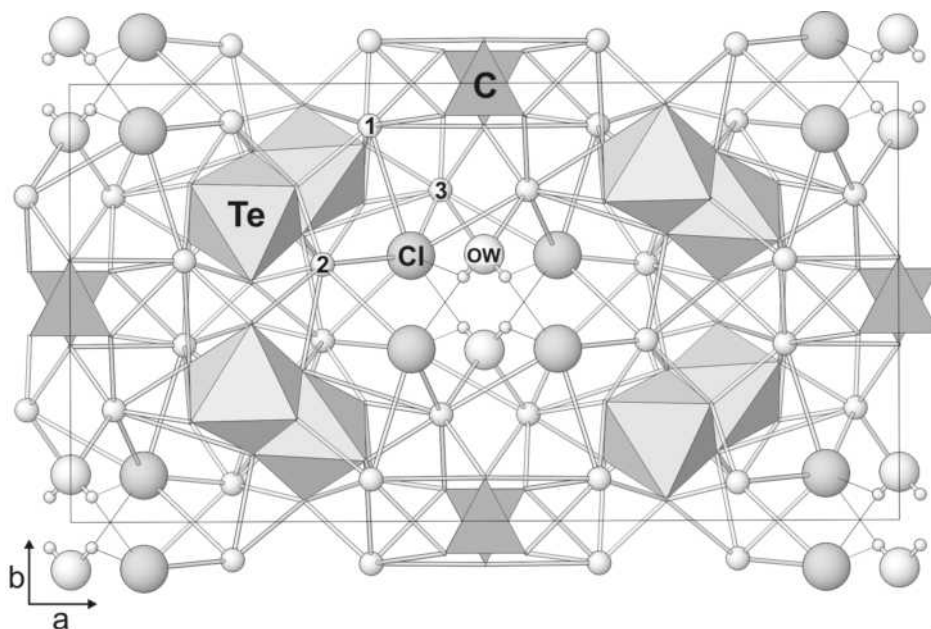


FIGURE 4. Structure of thorneite viewed down *c*. Numbered spheres are Pb atoms (Pb1, Pb2 and Pb3). Smallest spheres associated with OW are H atoms.

(Kampf et al. 2010d); and paratimroseite, 1.926 Å (Kampf et al. 2010d); however, the TeO₆ octahedron exhibits significant distortion, attributable to the repulsion between the Te⁶⁺ cations across the O7-O7 shared edge of the dimer. Te-O distances vary from 1.889 to 1.979 Å, O-Te-O angles vary from 77.3 to 100.9° and O-O distances vary from 2.469 to 2.923 Å. The Te-O7 distances are the longest, the O7-Te-O7 angle is the smallest and the O7-O7 edge is the shortest. The edge-sharing octahedral tellurate dimer, [Te₂⁶⁺O₁₀]⁸⁻, has not yet been found in any other mineral structure; however, it has been reported in synthetic compounds, cf. K₄[Te₂⁶⁺O₆(OH)₄](H₂O)_{7.3} (Lindqvist and Lundgren 1966), Na₂K₄[Te₂⁶⁺O₈(OH)₂](H₂O)₁₄ (Lindqvist 1969), and Na₄TeO₅ (Untenecker and Hoppe 1987). Similar octahedral distortions related to Te⁶⁺ repulsions occur in all of these structures.

The Pb atoms have lopsided nine- and tenfold coordinations (Fig. 5) attributable to the 6s² lone-electron-pair effect typically exhibited by Pb²⁺ (e.g., Moore 1988; Cooper and Hawthorne 1994; Kharisun et al. 1997; Mills et al. 2009). In fact, the Pb atoms in the structures of all seven recently discovered new minerals from Otto Mountain exhibit this effect.

The two equivalent H atoms of the OW group form bifurcated H bonds to two equivalent Cl sites (shown in Fig. 4). The H bonds are relatively long (2.68 and 2.71 Å), leaving OW relatively

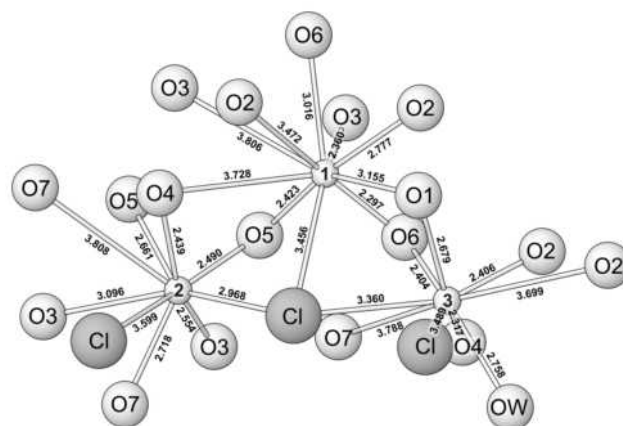


FIGURE 5. Coordinations of the Pb1, Pb2, and Pb3 atoms in thorneite. The lopsided distributions of bond lengths are attributable to the localization of the lone-pair electrons. Bond lengths are given in angstroms.

oversaturated. The 0.25 H atom associated with the 0.25 O at the Cl site may participate in an H bond to OW, but based upon the shortest Cl-OW bond length (3.175 Å) this would contribute a bond strength of about 0.005 valence units.

ACKNOWLEDGMENTS

We thank Associate Editor G. Diego Gatta, Technical Editor Ronald C. Petersen, referees Elena Sokolova and Filippo Vurro, and Stuart J. Mills for helpful comments on the manuscript. The Raman studies were conducted in the laboratory of George R. Rossman at the California Institute of Technology and with his assistance. The EMP analyses were supported by a grant to the California Institute of Technology from the Northern California Mineralogical Association. The remainder of this study was funded by the John Jago Trelawney Endowment to the Mineral Sciences Department of the Natural History Museum of Los Angeles County.

REFERENCES CITED

- Altomare, A., Cascarano, G., Giacobozzo, C., Guagliardi, A., Burla, M.C., Polidori, G., and Camalli, M. (1994) SIR92—A program for automatic solution of crystal structures by direct methods. *Journal of Applied Crystallography*, 27, 435.
- Brese, N.E. and O’Keeffe, M. (1991) Bond-valence parameters for solids. *Acta Crystallographica*, B47, 192–197.
- Brown, I.D. and Altermatt, D. (1985) Bond-valence parameters from a systematic analysis of the inorganic crystal structure database. *Acta Crystallographica*, B41, 244–247.
- Cooper, M. and Hawthorne, F.C. (1994) The crystal structure of wherryite, $\text{Pb}_2\text{Cu}_2(\text{SO}_4)_4(\text{SiO}_3)_2(\text{OH})_2$, a mixed sulfate-silicate with $[\text{PbM}(\text{TO}_3)_2\Phi]$ chains. *Canadian Mineralogist*, 32, 373–380.
- Cooper, M.A., Hawthorne, F.C., and Back, M.E. (2008) The crystal structure of khinite and polytypism in khinite and parakhinite. *Mineralogical Magazine*, 72, 763–770.
- Grice, J.D. and Roberts, A.C. (1995) Frankhawthorneite, a unique HCP framework structure of a cupric tellurate. *Canadian Mineralogist*, 33, 649–653.
- Grice, J.D., Groat, L.A., and Roberts, A.C. (1996) Jensenite, a cupric tellurate framework structure with two coordinations of copper. *Canadian Mineralogist*, 34, 55–59.
- Holland, T.J.B. and Redfern, S.A.T. (1997) Unit cell refinement from powder diffraction data: the use of regression diagnostics. *Mineralogical Magazine*, 61, 65–77.
- Kampf, A.R., Rossman, G.R., and Housley, R.M. (2009) Plumbophyllite, a new species from the Blue Bell claims near Baker, San Bernardino County, California. *American Mineralogist*, 94, 1198–1204.
- Kampf, A.R., Housley, R.M., Mills, S.J., Marty, J., and Thorne, B. (2010a) Lead-tellurium oxysalts from Otto Mountain near Baker, California: I. Ottoite, Pb_2TeO_5 , a new mineral with chains of tellurate octahedra. *American Mineralogist*, 95, 1329–1336.
- Kampf, A.R., Marty, J., and Thorne, B. (2010b) Lead-tellurium oxysalts from Otto Mountain near Baker, California: II. Housleyite, $\text{Pb}_8\text{CuTe}_4\text{O}_{18}(\text{OH})_2$, a new mineral with Cu-Te octahedral sheets. *American Mineralogist*, 95, 1337–1343.
- Kampf, A.R., Mills, S.J., Housley, R.M., Marty, J., and Thorne, B. (2010c) Lead-tellurium oxysalts from Otto Mountain near Baker, California: IV. Markcooperite, $\text{Pb}_2(\text{UO}_2)\text{Te}^{6+}\text{O}_6$, the first natural uranyl tellurate. *American Mineralogist*, 95, 1554–1559.
- (2010d) Lead-tellurium oxysalts from Otto Mountain near Baker, California: V. Timroseite, $\text{Pb}_2\text{Cu}_3^{2+}(\text{Te}^{6+}\text{O}_6)_2(\text{OH})_2$, and paratimroseite, $\text{Pb}_2\text{Cu}_4^{2+}(\text{Te}^{6+}\text{O}_6)_2(\text{H}_2\text{O})_2$, two new tellurates with Te-Cu polyhedral sheets. *American Mineralogist*, 95, 1560–1568.
- (2010e) Lead-tellurium oxysalts from Otto Mountain near Baker, California: VI. Telluroperite, $\text{Pb}_3\text{Te}^{4+}\text{O}_4\text{Cl}_2$, the Te analog of perite and nadorite. *American Mineralogist*, 95, 1569–1573.
- Kharisun, Taylor, M.R., Bevan, D.J.M., Rae, A.D., and Pring, A. (1997) The crystal structure of mawbyite, $\text{PbFe}_2(\text{AsO}_4)_2(\text{OH})_2$. *Mineralogical Magazine*, 61, 685–691.
- Kraus, W. and Nolze, G. (1996) POWDER CELL—A program for the representation and manipulation of crystal structures and calculation of the resulting X-ray powder patterns. *Journal of Applied Crystallography*, 29, 301–303.
- Krivovichev, S.V. and Brown, I.D. (2001) Are the compressive effects of encapsulation an artifact of the bond valence parameters? *Zeitschrift für Kristallographie*, 216, 245–247.
- Lindqvist, O. (1969) The crystal structure of the tellurate $\text{Na}_3\text{K}_4[\text{Te}_2\text{O}_8(\text{OH})_2](\text{H}_2\text{O})_4$. *Acta Chemica Scandinavica*, 23, 3062–3070.
- Lindqvist, O. and Lundgren, G. (1966) The crystal structure of potassium tellurate (VI). *Acta Chemica Scandinavica*, 20, 2138–2155.
- Mandarino, J.A. (1981) The Gladstone-Dale relationship. IV. The compatibility concept and its application. *Canadian Mineralogist*, 19, 441–450.
- Margison, S.M., Grice, J.D., and Groat, L.A. (1997) The crystal structure of leisingite, $(\text{Cu}^{2+}, \text{Mg}, \text{Zn})_2(\text{Mg}, \text{Fe})\text{Te}^{6+}\text{O}_6 \cdot 6\text{H}_2\text{O}$. *Canadian Mineralogist*, 35, 759–763.
- Mills, S.J., Kampf, A.R., Raudsepp, M., and Christy, A.G. (2009) The crystal structure of Ga-rich plumbogummite from Tsumeb, Namibia. *Mineralogical Magazine*, 73, 837–845.
- Moore, P.B. (1988) The joesmithite enigma: Note on the $6s^2\text{Pb}^{2+}$ lone pair. *American Mineralogist*, 73, 843–844.
- Sheldrick, G.M. (2008) A short history of SHELX. *Acta Crystallographica*, A64, 112–122.
- Untenecker, H. and Hoppe, R. (1987) Ein Neues Oxotellurat, Na_4TeO_5 , und eine Revision der Struktur von Li_4TeO_5 . *Journal of the Less-Common Metals*, 132, 79–92.

MANUSCRIPT RECEIVED JANUARY 28, 2010
 MANUSCRIPT ACCEPTED MAY 5, 2010
 MANUSCRIPT HANDLED BY G. DIEGO GATTA